UNB | Off-site Construction Research Centre

CSCE CSGC 1887 Canadian Society for Civil Engineering

Transforming Construction with Reality Capture Technologies:
The Digital Reality of Tomorrow

August 23-25, 2022, Fredericton, New Brunswick, Canada

AN EYE TRACKING BASED VIRTUAL TAPE MEASURE IN CONSTRUCTION

Wang, X[1], Han, W[1], Du, E.[2], Dai, F.[3], and Zhu, Z[1*]
[1] Department of Civil and Environmental Engineering, University of Wisconsin-Madison, USA
[2] Department of Civil and Coastal Engineering, University of Florida, USA
[3] Department of Civil and Environmental Engineering, West Virginia University, USA
[*] zzhu286@wisc.edu

Abstract: The metal tape measure is one of the most important tools used by construction workers on a daily basis. The measure allows the workers to make sure that their piece of work is completed correctly following designs and/or specifications. Therefore, it is a must-have item in the worker's toolkit. However, existing metal tape measures can be subject to manipulation difficulties, despite that they are durable, retractable, and affordable. A stake, marking flag, or second person is commonly required when measuring large areas. In addition, the metal hook or blade of the measure could injure the worker such as skin cuts. This research proposes a novel framework of virtual tape measures with an eye tracker and a stereo camera. The framework consists of three components: data collection for point-of-interest, sensor calibration and distance calculation. Specifically, the point-of-interest is generated when the worker stares at one location and closes his/her eyes for at least 1 second. Different kinds of data related to the point-of-interest are collected for further analysis. Then, the eye tracking device and stereo camera are calibrated from their captured images to obtain the transformed gaze point on the stereo camera image. Based on the transformed gaze point, the corresponding point cloud is extracted and unified for the distance measurement. The framework was tested by measuring dimensions of several elements. The measurements by the framework were compared with the tape measures to benchmark its accuracy. Results showed that the proposed method could perform the measures efficiently in a hands-free manner with an average absolute error of 2.8 cm.

Keywords: Tape measures; Eye tracking; Dimension measurement

1 INTRODUCTION

Every construction project is different, but they are all defined by the measurements that make up assets (e.g., the diameter of the drainage pipes required and the size of the plywood boards to cut). Therefore, taking accurate measurements plays an important role on ensuring that the construction projects run smoothly with the less amount of rework. It is not only the key foundation for the project success, but also the warranty of safety and quality for the work delivered (Mileseey Tools, 2021). Inaccurate measurement can always negatively affect the entire construction process, leading to additional cost and time, especially when the error is discovered after a project or phase has been completed on site. For example, a construction worker needs to measure the length of a pipe before it is cut. If the measurement is not correct, the worker's cutting action leads to an incorrect pipe to use. Then, the pipe cutting work must be redone to fix the error.

To help construction workers measure their piece of work and make sure that it is completed correctly following designs and/or specifications, different measuring tools and equipment have been developed, and the tape measure is one of the most important tools commonly used by construction workers for taking measurements (Robillard,2018). It is durable, retractable, and affordable. Compared with other tools, the tape measure is compact and can be easily carried from one location to another by tucking it into a work bag or clipping it onto the worker's belt. Also, it could come with different options, such as bold numbers and ultra bright blades for easy reading in low light (Keson Industries Inc., 2019). Considering all these benefits, the tape measure has become a must-have item in the worker's toolkit.

However, there are several disadvantages associated with the use of tape measures, especially metal tape ones. First, its measuring distance is limited, which is typically no more than 100 feet (Washington, 2015). When measuring a large area, a stake, marking flag, or second person is always required. Second, the use of metal tape measures easily ends up with potentially scratched fingers or skin cuts due to the metal hook or blade of the measure (Johnson, 2019). In addition, its compact format makes it possible to slip from the control of a worker and hit other workers. In 2014, a tragedy happened at a construction site in Jersey City, where a one-pound tape measure fell from the waist of a construction worker at a 50-story building; and the tape measure fell about 400 feet and hit and kill another construction worker below (Santora, 2014).

To address the limitations of traditional tap measures, the laser tape measures were developed. Also, the idea of using Augmented Reality for the virtual tape measures was explored. This research proposes a novel framework for conducting the virtual tape measures with an eye tracker and a stereo camera. The framework includes three components: data collection for point-of-interest, sensor calibration and distance calculation. Specifically, the point-of-interest is generated through eye gaze monitoring and different kinds of data related to the point-of-interest are collected. Further, the eye tracker and stereo camera are calibrated to get the transformed gaze point on the stereo camera image. Finally, the point cloud based on the transformed gaze point is extracted and unified for the distance measurement. The framework was tested by measuring dimensions of several built elements. Results showed that the proposed method could perform the measures efficiently in a hands-free manner. The average absolute measuring error is 2.8 cm.

2 RELATED WORK

2.1 Laser Tape Measures

A laser measure is a measuring device that relies on the time-of-flight or triangulation principle (Altuntas, 2021) to take the measurement. No matter what principle is adopted, the laser measuring device emits an eye-safe laser beam towards a target. When the laser beam hits the target's surface, it is reflected and received by the device. The time-of-flight principle considers that the velocity of the laser beam in air is constant, i.e., 300,000 km per second. Then, the distance between the device and the target could be calculated by counting the time that the laser beam takes to travel Under the triangulation principle, the location of the reflected laser beam is measured. The emitted laser beam and the reflected one form a triangle. Depending on the location of the reflected laser beam, the distance to the target is determined. Figure 1 illustrates both measurement principles.

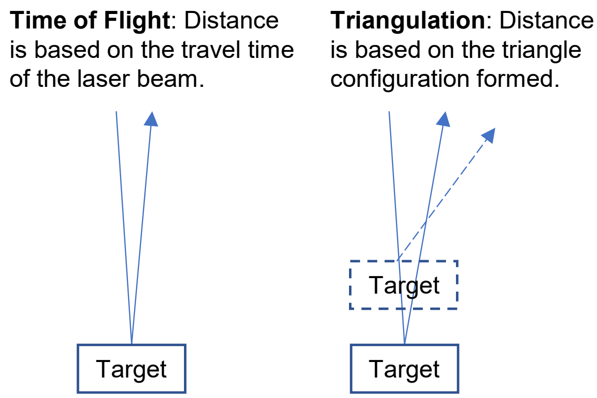

Figure 1: Time of flight and triangulation measurement principles

Compared with the traditional tape measures, the laser measures offer a greater measuring range as well as a higher measuring accuracy. They are convenient and safe to use due to the non-contact nature. For example, workers do not have to scramble up ladders to measure the height of ceilings. Also, they do not need to walk back and forth or have a second person at the other end when measuring the distance (Sebring, 2022). No matter how far the distance is, the measurement could be made as long as there is a line of sight to the target, and it is within range. In addition, existing laser measuring devices in the market typically provide simple functions for area and volume calculations (Dale and Scalisi, 2022). This way, a worker does not have to note the readings from the tape measures and then do the calculations on their own.

One major issue of the laser measures comes from the requirement that a target must be solid to reflect the laser beam. The reading will fail if the target's surface is not reflective. That is why it is always recommended to make multiple measurement to ensure the reading values are accurate and consistent especially when measuring the surface of a target is porous. Second, the emitted laser beam is sensitive to light and dust. As a result, measuring outdoor or in a hash environment becomes difficult. It is likely that the laser beam reflection is weak, and it is necessary to increase the laser intensity or install an extra solid flat reflective tape (Hermannová, 2021).

2.2 Virtual Tape Measures

Recently, the idea of the virtual tape measures has been proposed with the development of augmented and mixed reality technology. Augmented reality is the enhancement of a real-world environment with computer-generated perceptual information (Hayes, 2020). Mixed reality is the merging of real physical and virtual worlds, where both physical and digital objects could co-exist and interact with each other in real time (Milgram et al. 1994). Built upon existing smart phones (e.g., iPhone) and smart glasses (e.g., Microsoft Hololens), practitioners have created several applications for the virtual tape measures. For example, AirMeasure relies on the visual inertial odometry and measures the distance between two points in a three-dimensional space using the phone's built-in camera (Ro, 2017). Another example is HoloMeasure or MultiMeasure, either of which leverages the spatial map made by the HoloLens and could instantly calculate the exact distance between the marked points set by the user with air-taps (Rubino, 2016; Odom, 2017).

In academia, Huang et al. (2017) proposed a non-contact measurement method with interactive functions in the HoloLens. Under their method, the measurement space is scanned using the depth sensor on the HoloLens and the measurement points are determined using the gaze and gesture functions with the margin error of 10 mm (Huang et al. 2017). Loporcaro et al. (2019) evaluated the feasibility of using the HoloLens as a construction checking tool. It was noted that HoloLens tended to overestimate spatial dimensions in terms of measuring the length and the use of HoloLens had an average error of 87.7 mm with the physical tape and 22.1 mm with the virtual tape (Loporcaro et al. 2019).

In addition, the spatial mapping accuracy of the HoloLens has been recently evaluated under different environments. Terugi and Fassi (2022) presented a quantitative evaluation of the HoloLens 2 as a mapping instrument inside huge and complex monumental environments. Their evaluation results on three test areas in Milan Cathedral indicated that the largest deviation from the ground truth could reach 0.59 m (Terugi and Fassi, 2022). Hübner et al. (2019) evaluated the use of HoloLens for the mapping of indoor building environments. The results showed that the geometry of single rooms could be mapped, and the deviations are in the range of few centimeters for most parts of the rooms (Hübner et al. 2019). Also, Khoshelham et al. (2019) provided a geometric evaluation of 3D mesh data captured by the HoloLens for the indoor mapping. Their evaluation metrics includes local precision and global correctness. The results showed that the local precision of the HoloLens mesh was 2.25 cm, and the mesh was globally correct with a mean deviation of about 5 cm to the registered laser scanner point cloud and the 3D model (Khoshelham et al. 2019).

3 PROPOSED METHODOLOGY

This research proposes a novel framework of virtual tape measures with an eye tracker and stereo camera. The overview of the proposed framework is illustrated in Figure 2. The framework consists of three components: data collection for point-of-interest, sensor calibration, and distance calculation. Specifically, the point-of-interest is generated through the eye gaze point monitoring and different kinds of data (e.g. image from eye tracking device, point cloud from stereo camera) related to the point-of-interest are collected. Further, the eye tracking device and stereo camera are calibrated from their captured images to obtain the transformed gaze point into the stereo camera image. Based on the transformed gaze point, the corresponding point cloud is extracted and unified for the distance measurement. The details of these components are discussed in the following sections.

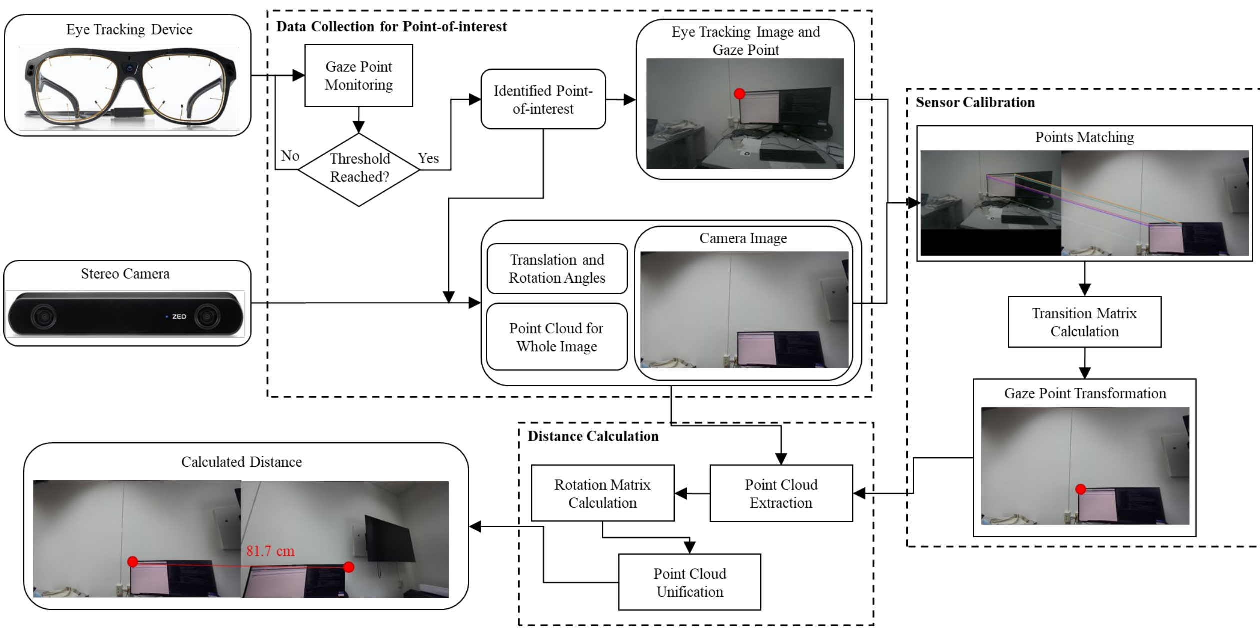

Figure 2: The overview of proposed framework

3.1 Data Collection for Point-of-interest

The purpose of this component is to generate the point-of-interest and then collect different kinds of data related to the generated point-of-interest from both eye tracking device and stereo camera. The point-of-interest is determined before the user closes his/her eyes for a duration. Specifically, the eye gaze points coming from the eye tracking device are continuously monitored. For the determination mechanism, when the gaze point of the user vanishes for a duration σ, the gaze point right before vanishing is determined as the point-of-interest and the moment that point was produced by the eye tracking device is recorded as

T. It should be noted that the selection of σ depends on how long the user needs to close his/her eyes to trigger the determination of point-of-interest. Here, σ has been set as 1 second.

Further, different kinds of data related to the generated point-of-interest are collected. These data come from two sensors: the eye tracking device and stereo camera. The eye tracking image at moment *T* and the point-of-interest (x_e, y_e) are obtained from the eye tracking device. For the stereo camera, the camera image, the point cloud for the whole image, and positional tracking parameters which are all captured at moment *T* are collected. The positional tracking parameters include the translation (t_x, t_y, t_z) and rotation angles (α, β, γ) of the stereo camera. The coordinate system of the stereo camera is shown in Figure 3. Here, t_x, t_y, t_z are translation values along *x*, *y* and *z* axis, separately. α, β, γ refer to yaw, pitch, and roll angles about *x*, *y* and *z* axis, respectively.

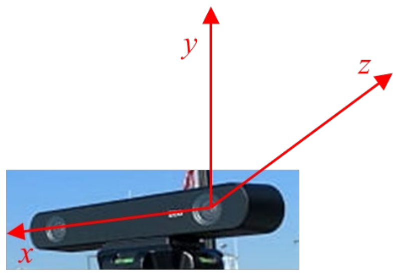

Figure 3: The coordinate system of stereo camera

3.2 Sensor Calibration

In this component, the eye tracking device and stereo camera are calibrated based on their captured images to transform the point-of-interest. This component can be divided into three steps: points matching between the eye tracking image and the camera image, transition matrix calculation, and point-of-interest transformation. For the points matching, Scale Invariant Feature Transform (SIFT) technique (Lowe, 2004) is employed to find the top K confident matching points between the eye tracking image ((x_{e1}, y_{e1}), … , (x_{eK}, y_{eK})) and the camera image ((x_{c1}, y_{c1}), … , (x_{cK}, y_{cK})). The SIFT algorithm (Lowe, 2004) firstly estimates a scale space extrema using the Difference of Gaussian (DoG). Then, the key point candidates are localized and refined by eliminating the low contrast points. Finally, a descriptor is employed to compute the local image description for each key point based on the image gradient magnitude and orientation to find top K confident matching points. In this study, K is set to be 20.

Based on the matching points, the transition matrix between the eye tracking image and the camera image is estimated through the projective transformation (Szeliski 2021). The relationship between a random pair of matching points (i = 1, 2, …, K) can be expressed through Eq. 1.

$$\begin{pmatrix} x_{ci} \\ y_{ci} \\ 1 \end{pmatrix} \equiv \begin{pmatrix} \widetilde{x_{c1}} \\ \widetilde{y_{c1}} \\ \widetilde{z_{c1}} \end{pmatrix} = \begin{pmatrix} h_{11} & h_{12} & h_{13} \\ h_{21} & h_{22} & h_{23} \\ h_{31} & h_{32} & h_{33} \end{pmatrix} \begin{pmatrix} x_{ci} \\ y_{ci} \\ 1 \end{pmatrix} = H \begin{pmatrix} x_{ei} \\ y_{ei} \\ 1 \end{pmatrix} \quad \text{(Eq. 1)}$$

where $H = \begin{pmatrix} h_{11} & h_{12} & h_{13} \\ h_{21} & h_{22} & h_{23} \\ h_{31} & h_{32} & h_{33} \end{pmatrix}$ is the transition matrix and $\sum h_{ij}^2 = 1$. In this study, the constrained least square method (Szeliski 2021) is employed to estimate the parameters of *H* that best observe all the matching points. It firstly constructs a matrix *A* regarding the matching points and then takes the smallest eigenvector of A^TA to estimate the transition matrix. More details about the constrained least square method could be found in the work of Szeliski (2021).

Further, the point-of-interest can be transformed from the eye tracking image to the camera image given the transition matrix. The transformed point on the camera image (x_c, y_c) is estimated using Eq. 2. After the transformation, the points-of-interest in the eye tracking image and their transformed ones in the camera images are expected to refer to the same location in the real-world space as shown in Figure 4.

$$\begin{pmatrix} x_c \\ y_c \\ 1 \end{pmatrix} \equiv \begin{pmatrix} \widetilde{x_c} \\ \widetilde{y_c} \\ \widetilde{z_c} \end{pmatrix} = \begin{pmatrix} h_{11} & h_{12} & h_{13} \\ h_{21} & h_{22} & h_{23} \\ h_{31} & h_{32} & h_{33} \end{pmatrix} \begin{pmatrix} x_e \\ y_e \\ 1 \end{pmatrix} \quad \text{(Eq. 2)}$$

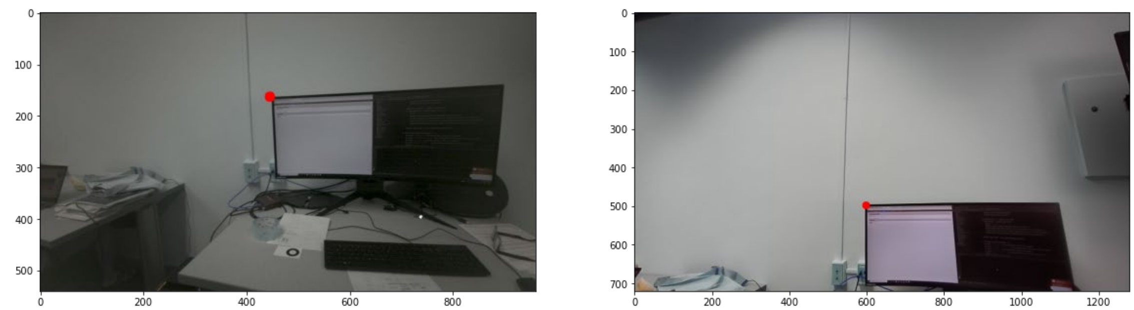

Figure 4: Transformation of points-of-interest on different images (left: eye tracking image; right: camera image)

3.3 Distance Calculation

The purpose of this component is to extract and unify the point cloud given the transformed point-of-interest in the camera image. Specifically, the 3D coordinate (x_p, y_p, z_p) of the transformed point-of-interest is firstly extracted from the whole point cloud based on their 2D coordinate (x_c, y_c). Then, the rotation matrix which reflects the current camera pose is established based on the rotation angles. The rotation matrix *R* can be derived from Eq. 3 (Arvo 1992).

$$R = R_x(\alpha)R_y(\beta)R_z(\gamma) = \begin{pmatrix} 1 & 0 & 0 \\ 0 & \cos\alpha & -\sin\alpha \\ 0 & \sin\alpha & \cos\alpha \end{pmatrix} \begin{pmatrix} \cos\beta & 0 & \sin\beta \\ 0 & 1 & 0 \\ -\sin\beta & 0 & \cos\beta \end{pmatrix} \begin{pmatrix} \cos\gamma & -\sin\gamma & 0 \\ \sin\gamma & \cos\gamma & 0 \\ 0 & 0 & 1 \end{pmatrix} \quad \text{(Eq. 3)}$$

Given the rotation matrix and translation, the 3D coordinate of the transformed point-of-interest can be unified through Eq. 4. The unified coordinate (x_u, y_u, z_u) is taking the global frame of the stereo camera as the basis.

$$\begin{pmatrix} x_u \\ y_u \\ z_u \end{pmatrix} = R \begin{pmatrix} x_p \\ y_p \\ z_p \end{pmatrix} + \begin{pmatrix} t_x \\ t_y \\ t_z \end{pmatrix} \quad \text{(Eq. 4)}$$

The whole framework terminates when it obtains the unified coordinates of two points-of-interest, which are the start and end point of the object the user intends to measure, separately. Then, the Euclidean distance between the unified coordinates of these two points is calculated as the final output.

4 RESULTS

4.1 Implementation

Figure 4 indicates the protype of the integrated sensors. The user was wearing an eye tracking glasses and a stereo camera is mounted on the head of the user through a head strap. Tobii Glasses 3 (Tobii Inc. 2021) was employed to get the eye tracking images and track the eye gaze points. A scene camera is mounted on the front of the glasses to get the first-person view frames. Two eye cameras are facing towards each eye, to obtain the eye gaze points. Besides, the ZED 2 stereo camera (Stereolabs 2019) was selected. The camera does not only provide stereo images but also generate the corresponding point cloud based on the stereo images. Also, the ZED camera is featured with the visual tracking of its surroundings to understand the movement of the user or system holding it. As the camera moves in the real world, it reports its new position and rotation with six degrees of freedom (6DoF).

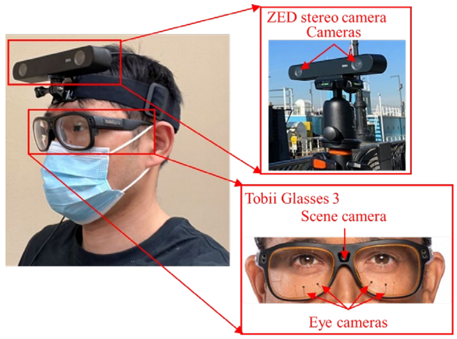

Figure 4: Protype of the integrated sensors

4.2 Test Results

A laboratory study was conducted to test whether the proposed framework could be used to measure the dimensions of different objects. These objects include two boxes, one computer screen, and one desk. Specifically, the user was asked to stare at the start point of an object he/she intended to measure and closed his/her eyes for at least 1 second. Then, the user would stare at the end point of the object and close his/her eyes for another second. During this process, the corresponding data would be captured by the eye tracking device and the stereo camera. Then, the dimension of the object which the user intended to measure was calculated.

Table 1 shows the matching of the key points and the transformation of the points of interest (i.e., start and end points) in two measuring examples. One was to measure the length of a computer screen and the other was to measure the length of a desk. The results in Table 1 indicated that the key points in the eye tracking images and the camera images were correctly generated and matched. Also, the points of interest in each example were referring to the same location in the real-world space.

Table 2 compiled the measurements made by the proposed framework, which were future compared with the measurements made by a metal tape. The measurements for the screen length, desk length, desk height, black box length, and yellow box length are around 81.7 cm, 132.5 cm, 72.8 cm, 64.8 cm, and 57.4 cm, separately. The results from the ruler are regarded as ground truth in this study. The absolute errors for these five test cases are 0.3 cm, 8.0 cm, 0.1 cm, 3.1 cm, and 2.6 cm, respectively. The average error is 2.8 cm.

5 DISCUSSION

Two lessons were learned from the laboratory experiment. First, the estimation of points of interest impacts the measure performance in the proposed framework. Taking the test case of measuring the yellow box length as an example, Figure 5 shows the captured points of interest before and after transformation. The estimation of the start point deviates from the left-top corner of the yellow box and was located closer to the end point, which would make the measured distance between the start and end point shorter than the actual yellow box length. The inaccurate estimation may be caused by the movements of closing eyes because they may affect the stability of eye gaze points.

Second, the transition matrix in the sensor calibration is another factor affecting the performance of the proposed framework. The found matching points may contain outliers, which easily influence the computation of transition matrix. In the example of measuring desk length as shown in Table 1, the start point after the transformation is slightly lower than the start point before the transformation. This makes the measured distance longer than the ground truth.

Table 1: Examples of distance measure results

		Screen		Desk	
	Functions	Eye tracking images	Camera images	Eye tracking images	Camera images
Start point	Matching	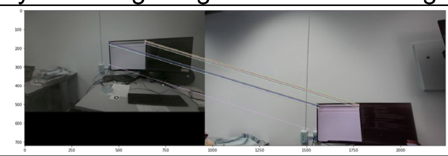		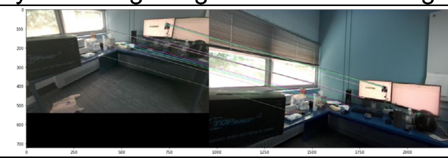	
	Transformation	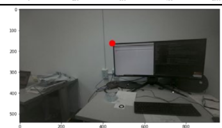	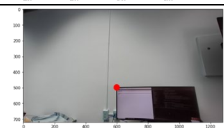		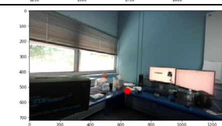
End point	Matching	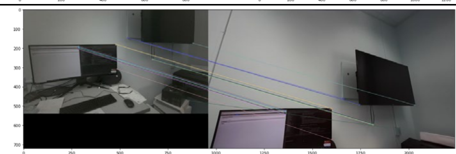		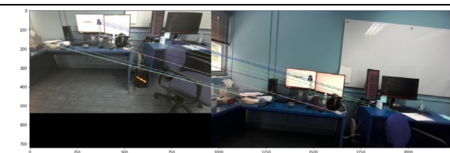	
	Transformation	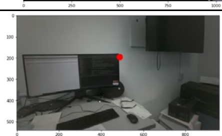			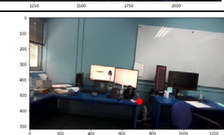

Table 2: Comparison of distance measure results

	Screen length (cm)	Desk length (cm)	Desk height (cm)	Black box length (cm)	Yellow box length (cm)
Measurements made by Ruler	81.4	124.5	73.4	61.7	60.0
Measurements made by the proposed framework	81.7	132.5	72.8	64.8	57.4
Absolute error	0.3	8.0	0.6	3.1	2.6
Relative error	0.37%	6.43%	0.82%	5.02%	4.33%

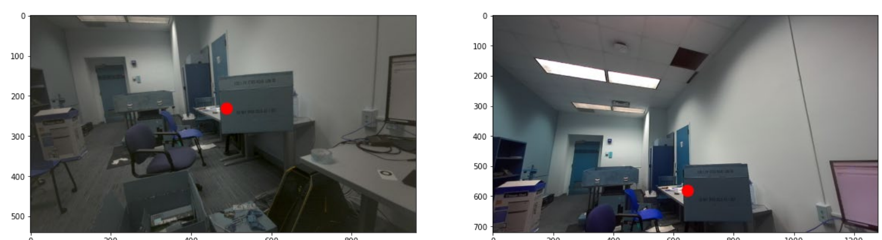

(a) Start point (left: Tobii; right: ZED)

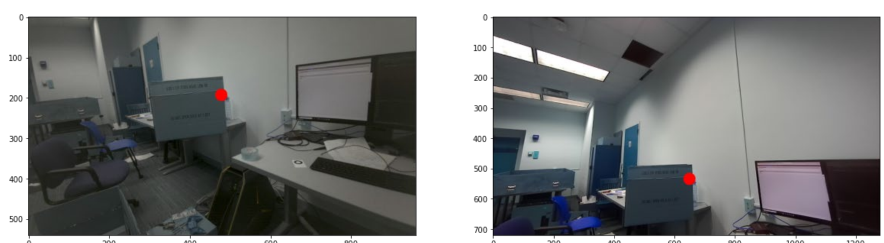

(b) End point (left: Tobii; right: ZED)

Figure 5: Points-of-interest before and after transformation for measuring yellow box length

6 CONCLUSION AND FUTURE WORK

This research presented a novel framework that relies on an eye tracker and a stereo camera for virtual tape measures. The framework includes three components: data collection for point-of-interest, sensor calibration, and distance calculation. It was tested in the indoor environments for measuring the size of computer screen, desk, and box. The test results indicated that the absolute error is in the range of 0.3 ~ 8.0 cm with an average of 2.8 cm. Although the measuring accuracy needs to be further improved, the proposed framework provided an efficient way to take the measurements in a hands-free manner. Future work will focus on reducing the errors introduced in the estimation of points of interest and the sensor calibration to improve the measurement accuracy.

7 ACKNOWLEDGEMENT

This research was supported by the Wisconsin Alumni Research Foundation via grant # AAJ4872.

8 REFERENCES

Arvo, J. 1992. Fast random rotation matrices. In: *Graphics Gems III (IBM Version)*. https://doi.org/10.1016/b978-0-08-050755-2.50034-8.

Altuntas, C. 2021. Triangulation and time-of-flight based 3D digitization techniques of culture heritage structures.", Int. Arch. Photogramm. Remote Sens. Spatial Inf. Sci., XLIII-B2-2021, 825–830, https://doi.org/10.5194/isprs-archives-XLIII-B2-2021-825-2021, 2021.

Dale, T. and Scalisi, T. 2022. The best laser measures of 2022. https://www.bobvila.com/articles/best-laser-measure/ (June 24, 2022).

Hayes, A. 2020. Augmented reality. https://www.investopedia.com/terms/a/augmented-reality.asp (June 23, 2022).

Hermannová, A. 2021. Advantages and disadvantages of laser distance meters - are they worth it? https://www.measuritec.com/blogs/news/advantages-and-disadvantages-of-laser-distance-meters-are-they-worth-it (June 23, 2022).

Huang, J., Yang, B. and Chen, J. (2017). "Non-contact Measurement Method Research Based on HoloLens," 2017 International Conference on Virtual Reality and Visualization (ICVRV), 2017, pp. 267-271, doi: 10.1109/ICVRV.2017.00061.

Hübner, P., Landgraf, S., Weinmann, M., and Wursthorn, S. 2019. Evaluation of the Microsoft HoloLens for the mapping of indoor building environments. Dreiländertagung der DGPF, der OVG und der SGPF in Wien, Österreich – Publikationen der DGPF, Band 28, 2019

Johnson, S. 2019. The advantage and disadvantages of tape measures. https://www.ehow.com/list_6735942_advantages-disadvantages-tape-measures.html (June 24, 2022).

Keson Industries Inc. 2019. A guide to construction measuring tools. https://www.keson.com/a-guide-to-construction-measuring-tools/ (June 23, 2022).

Khoshelham, K., Tran, H., and Acharya, D. 2019. Indoor Mapping Eyewear: Geometric Evaluation of Spatial Mapping Capability of HoloLens. Int. Arch. Photogramm. Remote Sens. Spat. Inf. Sci. 2019, XLII-2/W13, 805–810.

Loporcaro G., Bellamy L., McKenzie, P., Riley, H. and Ralston, S. 2019. Evaluation of Microsoft Hololens augmented realty technology as a construction checking tool. https://ir.canterbury.ac.nz/handle/10092/101484 (June 24, 2022).

Lowe, D. 2004. Distinctive image features from scale-invariant keypoints. International Journal of Computer Vision 60, 91–110.

Mileseey Tools, 2021. Top 5 benefits of using a general laser tape measure in building construction. https://www.mileseeytools.com/blogs/news/top-5-benefits-of-using-a-general-laser-tape-measure-in-building-construction (June 19, 2022).

Milgram, Paul & Kishino, Fumio. 1994. A Taxonomy of Mixed Reality Visual Displays. IEICE Trans. Information Systems. vol. E77-D, no. 12. 1321-1329.

Odom, J. 2017. New Spatial Map Measuring Tool & Beating Heart App for HoloLens. https://hololens.reality.news/news/have-you-seen-this-new-spatial-map-measuring-tool-beating-heart-app-for-hololens-0175832/ (June 24, 2022).

Ro, L. 2017. AR Measure turns your phone into a virtual measuring tape. https://archive.curbed.com/2017/6/29/15894556/ar-measure-app-augmented-reality-ruler-measuring-tape-ios (June 24, 2022).

Robillard, R. 2018. Best tape measure. https://www.toolboxbuzz.com/head-to-head/best-tape-measure/ (June 24, 2022).

Santora, M. 2014. Falling tape measure kills man at Jersey City construction site. https://www.nytimes.com/2014/11/04/nyregion/falling-tape-measure-kills-man-at-jersey-city-construction-site.html (June 22, 2022).

Sebring, B. 2022. 7 Best laser tape measure tools [2022 reviews]. https://sebringdesignbuild.com/best-laser-tape-measure-review/ (June 23, 2022).

Stereolabs. 2019. ZED 2-AI Stereo Camera. 2019. https://www.stereolabs.com/zed-2/ (June 23, 2022).

Rubino, D. 2016. Microsoft's HoloLens gets a virtual tape measure to let you get the size of anything you see. https://www.windowscentral.com/hololens-gets-virtual-tape-measure (June 24, 2022).

Szeliski, R. 2021. Computer Vision : Algorithms and Applications 2nd Edition. *Springer*.

Teruggi, S. and Fassi, F. 2022. HoloLens 2 spatial mapping capabilities in vast monumental heritage environments. The International Archives of the Photogrammetry, Remote Sensing and Spatial Information Sciences. XLVI-2/W1-2022. 489-496. 10.5194/isprs-archives-XLVI-2-W1-2022-489-2022.

Tobii Inc. 2021. Tobii Pro Glasses 3. 2021. https://www.tobiipro.com/product-listing/tobii-pro-glasses-3/ (June 23, 2022).

Washington, S. 2015. The pros and cons of measuring devices. https://thescoop.cisgroup.net/blog/the-pros-and-cons-of-measuring-devices (June 23, 2022).